Inorganic Chemistry

Communication

pubs.acs.org/IC

Switchable Phase Behavior of [HBet][Tf_2N]–H_2O upon Neodymium Loading: Implications for Lanthanide Separations

Daniel P. Fagnant, Jr.,[†] George S. Goff,*[,‡] Brian L. Scott,[§] Wolfgang Runde,[∥] and Joan F. Brennecke*[,†]

[†]Department of Chemical and Biomolecular Engineering, University of Notre Dame, 182 Fitzpatrick Hall, Notre Dame, Indiana 46556, United States

[‡]Chemistry Division, [§]Material Physics and Applications Division, and [∥]Science Program Office, Los Alamos National Laboratory, Los Alamos, New Mexico 87545, United States

Supporting Information

ABSTRACT: Task-specific ionic liquids (TSILs) present an opportunity to replace traditional organic solvents for metal dissolution or separation. To date, a thorough investigation of the physical properties of biphasic TSIL–H_2O systems and the effects of metal loading is lacking. In this work, the change in the liquid–liquid equilibrium of [HBet][Tf_2N]–H_2O upon the addition of Nd(III) is investigated by cloud-point measurements. The addition of Nd(III), drops the upper critical solution temperature by over 20 °C. Further investigation of the [HBet][Tf_2N]–Nd(III) system led to the formation of single crystals of $[Nd_2(H_2O)_8(\mu_2\text{-Bet})_2(\mu_3\text{-Bet})_2][(Cl)_2(Tf_2N)_4]$ from the TSIL phase.

Room-temperature ionic liquids (ILs) are liquid salts with melting points below 100 °C. ILs can be applied to a wide range of applications by taking advantage of their varying properties such as viscosity, density, and solubility. Recent reviews have highlighted applications for ILs in areas such as solvent extraction, electrodeposition, and catalysis.[1] One application that has attracted increased interest is the use of ILs for separation in advanced nuclear fuel cycles.[2−4] Solvent extraction is one of the primary techniques for the purification of radionuclides, and ILs are strong candidates to replace conventional organic solvents. While the solubility of metals in noncomplexing ILs is generally poor, task-specific ILs (TSILs) can be designed by incorporating functional groups into the IL cation or anion. For example, Nockemann et al. suggested (trimethylammonio)acetate bis((trifluoromethyl)sulfonyl)imide, also known as betaine bis(triflimide) or [HBet][Tf_2N], for the solubilization of metal oxides and salts.[5] This TSIL greatly increased the solubility of a range of transition-metal salts and oxides, including uranium and the lanthanides. Additional amino-based carboxyl-functionalized ILs have been studied, and a number of crystal structures were isolated for several f element and transition metals.[6−8]

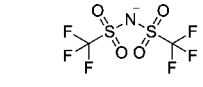

bis((trifluoromethyl)sulfonyl)amide

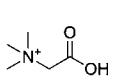

Betaine

One interesting property of [HBet][Tf_2N] is its significant solubility with H_2O. Nockemann et al. reported that the liquid–liquid equilibrium (LLE) of [HBet][Tf_2N] and H_2O has an upper critical solution temperature (UCST), with the two components being miscible in all compositions above 55.5 °C.[5] The temperature-dependent miscibility with H_2O provides several advantages for separations processes: (1) H_2O is known to alter the solvation properties and increase dissolution kinetics, (2) higher UCSTs generally increase solubility and dissolution kinetics, (3) better mixing can be achieved during dissolution with a single-phase system, and (4) cooling to two phases concentrates the metal in the IL phase (Figure 1).

Figure 1. Neodymium(III) preconcentrated in [HBet][Tf_2N] at room temperature and miscible with water at elevated temperature.

For development of a [HBet][Tf_2N]-based extraction process, it is necessary to understand how the physical properties change with temperature and composition. Several pure-component properties for [HBet][Tf_2N] have previously been reported. Nockemann et al. reported a melting point of 57 °C and density and viscosity at 60 °C of 1.531 g cm^{-3} and 351 cP, respectively.[5] Our thermal analysis of [HBet][Tf_2N] indicates a glass transition temperature (T_g) of −39 °C, a melting point of 54 °C, and a decomposition temperature (T_{onset}) of 325 °C, which is comparable to the thermal gravimetric analysis reported by Rao et al.[9] The pure-component density at 65 °C was determined to be 1.54 g cm^{-3}, which matches the previously reported value.[5] The viscosity of [HBet][Tf_2N] (with less than 100 ppm of H_2O and halide) was measured from 65 to 100 °C (see the Supporting Information) and fit to the Vogel–Fulcher–Tammann (VFT) equation (eq 1)

$$\eta(T) = \eta_0 \exp[B/(T - T_g)] \quad (1)$$

where η_0 = 1.099 cP, B = 510 °C, T_g = −39 °C, and R^2 = 0.9998.

The viscosity of 147 cP, measured in this work at 65 °C, is considerably lower than the previously reported value of 351 cP,[5]

Received: October 29, 2012
Published: January 4, 2013

   dx.doi.org/10.1021/ic302359d | Inorg. Chem. 2013, 52, 549−551

and extrapolation of the VFT fit to 60 °C significantly underpredicts the viscosity. Our viscosity measurements at 60 °C did not provide reliable results because the temperature is too close to the melting point. Seddon et al. have shown Cl^- impurities can greatly increase viscosity.[10] Nockemann et al. used the silver nitrate test to measure Cl^- impurities, which has a higher limit of detection than ion chromatography and is complicated by the ability of betaine to complex silver ions.[5] The effect of the water content on the density of [HBet][Tf_2N] was studied from 25 to 60 °C. The densities of pure [HBet][Tf_2N] and [HBet][Tf_2N]−H_2O mixtures decrease linearly with temperature, while the density of the mixtures decreases non-linearly with increasing water.

To measure the LLE of TSIL−H_2O mixtures, we utilized the cloud-point method, in which a single-phase solution is cooled while mixing until the first point of cloudiness is observed, indicating a phase split. The previously reported equilibrium measurements were performed using a gravimetric drying technique.[5] While the UCST measurements for the two methods show a qualitative agreement, there is a consistent shift of the phase envelope - to a higher weight percent of H_2O. This indicates that [HBet][Tf_2N] has a higher water solubility than previously reported by Nockemann et al.[5] Karl Fischer coulometric titration for the room-temperature solubility of H_2O in [HBet][Tf_2N] confirms the cloud-point measurements in this study (Figure 2). Differences

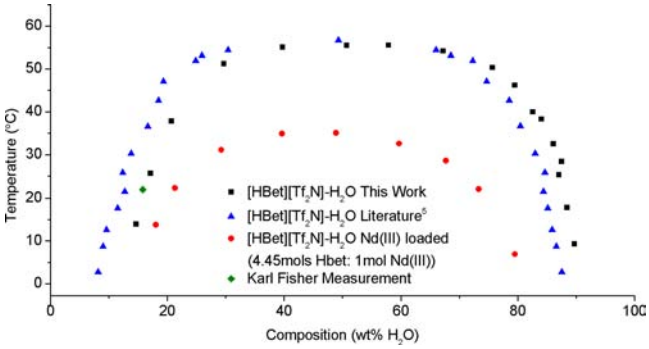

Figure 2. [HBet][Tf_2N]−H_2O LLE: This work and literature.[5]

between the measurement techniques are likely due to incomplete drying in the gravimetric technique.[5]

Because [HBet][Tf_2N] can solvate and complex metal ions, the effect of metal loading on the LLE must be understood for the design of a separation process. In Figures 2 and 3, we report for the first time the effect of Nd_2O_3 loading on the LLE of a TSIL−H_2O system. To quantify the change of the [HBet][Tf_2N]−H_2O−Nd LLE, cloud-point measurements were repeated at a constant [HBet][Tf_2N]:Nd ratio of 4.45:1. At this Nd(III) loading, the UCST decreases from 55.5 to 35.1 °C. In addition, the overall mutual solubility of the two phases increases, illustrated by a narrowing of the phase envelope (Figure 2). This change in the UCST and LLE with high metal loading, which has not been reported previously, is an important factor for the design of a solvent extraction process.

The parabolic nature of the LLE phase envelope allows for the UCST to be estimated at a 50:50 weight composition mixture. To further demonstrate the drop in the UCST with metal loading, cloud-point temperatures of mixtures with equal masses of H_2O and Nd(III)-loaded [HBet][Tf_2N] were determined over a range of Nd(III) concentrations (Figure 3). The lowest UCST of 34.2 °C corresponds to a molar ratio of 4 mols of [HBet][Tf_2N] per mol of Nd(III). It has been previously

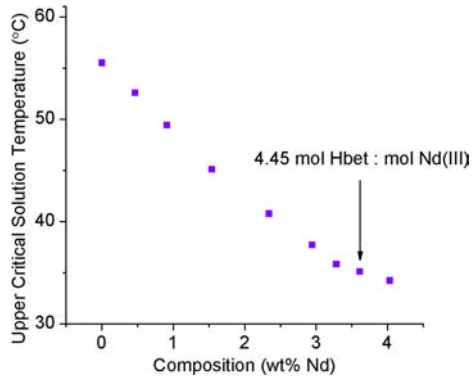

Figure 3. Dependence of the UCST for the 50:50 wt % ([HBet]-[Tf_2N]−Nd):H_2O solutions upon Nd_2O_3 loading.

reported that metal salts and oxides are soluble in [HBet][Tf_2N] up to stoichiometric ratios (up to 4:1), as found in crystal structures for lanthanide [HBet][Tf_2N] complexes.[5,7,11]

Three different structure types have previously been reported for [HBet][Tf_2N]−lanthanide complexes.[5,7,11] These complexes all exhibit a 4:1 stoichiometry of HBet to Ln and were isolated from aqueous solutions by reacting lanthanide oxides or chlorides with [HBet][Tf_2N], followed by recrystallization from H_2O. We isolated from the TSIL a new Nd(III)-HBet complex with a 2:1 ligand-to-metal stoichiometry. $[Nd_2(H_2O)_8(\mu_2\text{-Bet})_2(\mu_3\text{-Bet})_2]$-$[Cl_2(Tf_2N)_4]$ (**I**) was synthesized by dissolving $NdCl_3{\cdot}6H_2O$ into the H_2O-saturated TSIL phase and slowly evaporating water at room temperature. Small rectangular plates of **I** were isolated and characterized by single-crystal X-ray diffraction. Figure 4 shows the

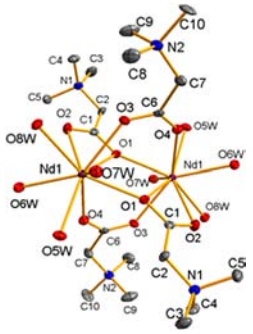

Figure 4. Thermal ellipsoid of the cationic unit of **I**.

thermal ellipsoid and atomic numbering scheme for the dimeric cationic unit of **I**; Table 1 lists selected bond lengths and angles.

Complex **I** crystallizes in the monoclinic space group $P2_1/n$. In the cationic unit, each neodymium atom is nine-coordinate with four bound water molecules and five coordinated carboxylate oxygen atoms from four betaine ligands to complete the monocapped distorted square-antiprismatic geometry around the metal. The structure of **I** is similar to those of $[Eu_2Bet_8(H_2O)_2]$-$[(Tf_2N)_4]$ (**II**) and $[Eu_2Bet_8(H_2O)_4][(Tf_2N)_4]$ (**III**),[7] which contain dimeric lanthanide cations connected by both μ^2- and μ^3-bridging betaine ligands. The μ^3-coordination mode for the bridging ligands is not present in $[Dy_2Bet_8(H_2O)_4][(Tf_2N)_4]$ (**IV**).[5] The bond lengths for Nd−O in **I** vary from 2.454(4) to 2.631(3) Å, where the shortest bonds are the bidentate bridging betaine carboxyl groups (O3 and O4) and the longest bonds are the μ^3-bridging oxygen atom (O1). The Nd−OW bonds vary from 2.478(3) to 2.518(3) Å, which is longer than the

dx.doi.org/10.1021/ic302359d | Inorg. Chem. 2013, 52, 549−551

Table 1. Selected Bond Lengths and Angles for I

Nd1−O1	2.631(3)	Nd1−O5W	2.478(3)
Nd1−O2	2.518(3)	Nd1−O6W	2.497(3)
Nd1−O3	2.454(4)	Nd1−O7W	2.518(3)
Nd1−O4	2.446(4)	Nd1−O8W	2.478(3)
O1−Nd1−O1	71.2(1)	O1−C1−O2	122.1(4)
O1−Nd1−O2	50.4(1)	O3−C6−O4	127.7(4)
O3−Nd1−O4	134.9(1)		

bidentate bridging Nd−O bonds but shorter than the μ^3-bridging bonds. The μ^3-oxygen atoms have a sharper bridging angle, 108.8°, compared to the bidentate bridging, 134.9°, for O3−Nd1−O4. The dimeric cations are surrounded by four Tf_2N^- and two Cl^- counterions in the lattice.

I is notably different from the reported structures because it has a lower stoichiometric ratio of HBet to Nd and it contains both Cl^- and Tf_2N^- counteranions. In addition, some of the betaine ligands have been replaced by coordinated H_2O molecules. Complexes **II**−**IV** all contain monodentate terminal betaine ligands, while complex **I** only contains bridging ligands. Metal-to-metal distances in the dimers are 4.0989(4), 4.0210(2), 4.1080(7), and 4.4271(3) Å for complexes **I**−**IV**, respectively. The Ln−Ln distance in **IV** is greater due to the absence of μ^3-bridging ligands.

Previous work with betaine zwitterions in acidic solutions has yielded complexes with both 4:1 and 2:1 betaine:Ln(III) stoichiometries. $[Eu_2Bet_4(H_2O)_8]Cl_6{\cdot}6H_2O$ (**V**) was crystallized from HCl with a dissolved betaine zwitterion.[11] The stoichiometry and coordination geometry of the cationic unit of **V** are the same as in **I**, which was isolated from an IL. Despite similar coordination geometries, **V** crystallized in the more ordered orthorhombic crystal system compared to the monoclinic system of **I**, which has a distorted monocapped square-antiprismatic geometry.

The existence of several compounds with varying stoichiometric ratios of H_2O to betaine indicates that there is a dynamic competition between betaine and water for lanthanide coordination. It is noteworthy that the dimeric lanthanide moiety with bridging ligands remains intact while the terminal betaine ligands can be replaced by H_2O.

Additional spectroscopic characterization of complex **I** redissolved in $[HBet][Tf_2N]$ is shown in Figure 5. The electronic

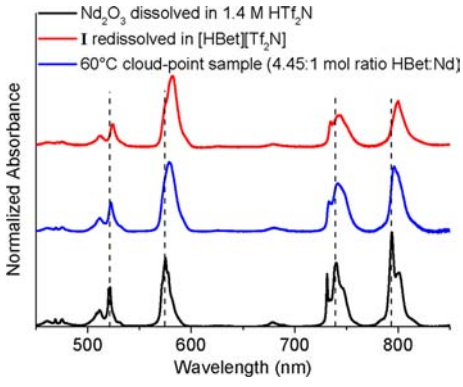

Figure 5. UV-vis comparison of various $[HBet][Tf_2N]$−H_2O−Nd samples.

absorbance spectrum for Nd(III) is characterized by a number of Laporte-forbidden f−f transitions in the visible region from 400 to 900 nm.[12] The prominent Nd(III) absorbances of **I** in $[HBet][Tf_2N]$ and in a single-phase cloud-point sample at 60 °C are shifted to higher wavelengths compared to Nd_2O_3 dissolved in 1.4 M HTf_2N. This suggests that Nd(III) is complexed with betaine in solution. Differences in the two Nd−TSIL samples could indicate the formation of different solution species, influenced by changes in the water content and temperature.

TSILs such as $[HBet][Tf_2N]$ exhibit characteristics that can be exploited for metal separation by utilizing unique temperature-dependent water miscibilities. In this work, we report for the first time the change in the LLE of an TSIL−H_2O system with metal loading. A large change in the UCST, as well as a decrease in the hydrophobicity of the TSIL phase, is observed. In addition, important physical parameters, such as the density and viscosity, for the design of a process have been developed and compared to existing data. The Nd(III) crystal structure obtained directly from $[HBet][Tf_2N]$ as opposed to aqueous dilution indicates integration of the lanthanide into the TSIL matrix. A full understanding of the actual solution speciation of lanthanides in $[Hbet][Tf_2N]$ is currently under investigation.

■ ASSOCIATED CONTENT

Ⓢ Supporting Information

X-ray crystallographic data in CIF format, experimental details, spectroscopic and physical property data. This material is available free of charge via the Internet at http://pubs.acs.org.

■ AUTHOR INFORMATION

Corresponding Author

*E-mail: jfb@nd.edu (J.F.B.), georgeg@lanl.gov (G.S.G.).

Notes

The authors declare no competing financial interest.

■ ACKNOWLEDGMENTS

The authors acknowledge the Los Alamos Laboratory Directed Research and Development Program at Los Alamos National Laboratory for financial support during this project. We also thank Yong Huang (Notre Dame) for thermal analysis.

■ REFERENCES

(1) Abbott, A. P.; Frisch, G.; Hartley, J.; Ryder, K. S. *Green Chem.* **2011**, *13*, 471−481.

(2) Vasudeva Rao, P. R.; Venkatesan, K. a.; Rout, a.; Srinivasan, T. G.; Nagarajan, K. *Sep. Sci. Technol.* **2012**, *47*, 204−222.

(3) Billard, I.; Ouadi, A.; Gaillard, C. *Anal. Bioanal. Chem.* **2011**, *400*, 1555−1566.

(4) Sun, X.; Luo, H.; Dai, S. *Chem. Rev.* **2012**, *112*, 2100−2128.

(5) Nockemann, P.; Thijs, B.; Pittois, S.; Thoen, J.; Glorieux, C.; Van Hecke, K.; Van Meervelt, L.; Kirchner, B.; Binnemans, K. *J. Phys. Chem. B* **2006**, *110*, 20978−20992.

(6) Nockemann, P.; Van Deun, R.; Thijs, B.; Huys, D.; Vanecht, E.; Van Hecke, K.; Van Meervelt, L.; Binnemans, K. *Inorg. Chem.* **2010**, *49*, 3351−3360.

(7) Nockemann, P.; Thijs, B.; Lunstroot, K.; Parac-Vogt, T. N.; Görller-Walrand, C.; Binnemans, K.; Van Hecke, K.; Van Meervelt, L.; Nikitenko, S.; Daniels, J.; Hennig, C.; Van Deun, R. *Chem.—Eur. J.* **2009**, *15*, 1449−1461.

(8) Nockemann, P.; Thijs, B.; Hecke, K. V.; Meervelt, L. V.; Binnemans, K. *Cryst. Growth. Des.* **2008**, *8*, 1353−1363.

(9) Rao, C. J.; Venkatesan, K. a.; Nagarajan, K.; Srinivasan, T. G. *Radiochim. Acta* **2008**, *96*, 403−409.

(10) Seddon, K. R.; Stark, A.; Torres, M.-J. *Pure Appl. Chem.* **2000**, *72*, 2275−2287.

(11) Yang, G.; Chen, H.; Zhou, Z.; Chen, X. *J. Chem. Crystallogr.* **1999**, *29*, 309−316.

(12) Carnall, W. T. *Handbook on the Physics and Chemistry of Rare Earths*; Elsevier BV: Amsterdam, The Netherlands, 1979; Vol. 3, p 171.